

MiR-135a regulates renal fibrosis in rats with diabetic kidney disease through the Notch pathway

L.-Y. ZHANG¹, Y. WANG², Y.-R. YANG¹, J.-J. SHAO¹, B. LIANG²

¹Department of Nephrology, The Second Hospital of Shanxi Medical University, Taiyuan, China

²Department of Cardiology, The Second Hospital of Shanxi Medical University, Taiyuan, China

Abstract. – **OBJECTIVE:** To explore the influence of micro ribonucleic acid (miR)-135a on the renal fibrosis in rats with diabetic kidney disease (DKD) through the Notch signaling pathway.

MATERIALS AND METHODS: A total of 30 male Wistar rats weighing 200-220 g were selected and randomly divided into Control group (n=10), diabetes mellitus (DM) group (n=10), and miR-13a inhibitor group (n=10). Streptozotocin (STZ) was intraperitoneally injected daily to establish the DM model in rats of both DM group and miR-135a group, while normal saline was given daily through intraperitoneal injection in rats of Control group. After 4 weeks, the rats in miR-135a inhibitor group were intraperitoneally injected with miR-135a inhibitor, and those in Control and DM groups were administrated with an equal amount of normal saline. Changes in the blood glucose (BG), glycated hemoglobin (GHb), serum creatinine (Scr), triglyceride (TG), and total cholesterol (TC) of rats were evaluated, and the pathological changes in the renal tissues of DM rats were observed via hematoxylin-eosin (HE) staining. Sirius red staining was performed to observe the changes in collagen fibers in the kidney of all groups of rats. The expressions of Notch and Hes1 in the renal tissues of rats in each group were detected using immunohistochemistry. Immunofluorescence assay was employed to detect the positive expression of Notch in the renal tissues of rats. The mRNA expressions of Notch and miR-135a were detected via quantitative Reverse Transcription-Polymerase Chain Reaction (qRT-PCR). Finally, Western blotting was conducted to detect the protein expressions of Notch, Notch intracellular domain (NICD) and Hes1.

RESULTS: Compared with Control group, rats in DM group had substantially raised levels of BG, GHb, Scr, TG, and TC ($p<0.05$). HE staining showed that the rats in Control group had renal tubular cells with normal morphology and well-defined structure, while those in DM group exhibited evident cavitation in the renal tubular

epithelium. Sirius red staining results manifested that the red collagen fibers were evenly distributed with light staining in the glomeruli and renal tubules of rats in Control group. In contrast, the collagen fibers of the glomeruli and renal tubules of rats in DM group exhibited deep and evident red staining. Moreover, compared with DM group, rats in miR-135a inhibitor group had notably faded red staining in the glomeruli and renal tubules of rats, evenly distributed collagen and remarkably decreased fibrotic nodules. According to immunohistochemistry detection results, the protein levels of Notch and Hes1 in the renal tubulointerstitial cells and renal tubular epithelial cells of rats in DM group were markedly higher than those in Control group. Compared with those in DM group, their protein levels were remarkably lowered in miR-135a inhibitor group ($p<0.05$). Immunofluorescence assay results revealed that the protein level of Notch in the renal tissues of rats in DM group was considerably higher than that in Control group ($p<0.05$), while its protein level in miR-135a inhibitor group was significantly lower than that in DM group. According to qRT-PCR results, compared with those in Control group, mRNA expressions of Notch mRNA and miR-135a in the rat kidney tissues were substantially raised in DM group ($p<0.05$), and they were notably lowered in miR-13a inhibitor group compared with those in DM group ($p<0.05$). Finally, Western blotting results manifested that the protein levels of Notch, NIC, and Hes1 in the renal tissues of rats in DM group were considerably higher than those in Control group ($p<0.05$), and that their protein expression levels in miR-135a inhibitor group were markedly lower than those in DM group ($p<0.05$).

CONCLUSIONS: Inhibition of miR-135a can reduce the renal fibrosis in DKD rats through the Notch pathway.

Key Words:

MiR-135a, Diabetes mellitus, Renal fibrosis, Notch, Signaling pathway.

Introduction

Diabetes mellitus (DM) is a chronic metabolic syndrome caused by insulin insufficiency, and diabetic kidney disease (DKD) is one of the most severe microvascular complications of DM¹. Approximately 40% of DM patients suffer from DKD, which has become the leading cause of end-stage nephropathy in developed countries². The major histopathological features of the early-stage DKD include mesangial cell proliferation and podocyte injury. Eventually, extracellular matrix (ECM) proteins are upregulated in the glomerular mesangium and renal tubulointerstitium, such as glomerulosclerosis and tubulointerstitial fibrosis³. Ma et al⁴ demonstrated that micro ribonucleic acids (miRNAs) help to reveal the pathogenesis of DKD.

MiRNAs are a class of small non-coding RNAs that can lower the expressions of the target genes, inducing changes in cell proliferation, apoptosis, and differentiation in mammal development⁵. Of note, they are stably present in human peripheral blood and can resist active RNases⁶. Dong et al⁷ manifested that the expression profile of miRNAs can be altered in various disease states, and that serum miRNAs can be detected to confirm the diagnosis of diseases. Based on the findings in some studies, serum miR-135a is substantially raised in DKD patients. Jefferson et al⁸ proved that the level of miR-135a is up-regulated in many types of cancers. Ding and Choi⁹ corroborated that miR-135a is elevated in human skeletal muscle in DM, and that *in vivo* silencing miR-135a alleviates hyperglycemia and improves glucose tolerance. It was found by consulting the genomic database in University of Southern California that pre-miR-135a is located on human chromosome 3¹⁰. The above results suggested that miR-135a may be the characteristic miRNA of DKD.

Although Notch is associated with diverse diseases in organisms, its role in the renal fibrosis in DM rats has been rarely reported. The present research explored the role of miR-135a in influencing renal fibrosis in DM through the Notch signaling pathway, thereby providing a certain experimental basis for the treatment of DM induced-renal fibrosis.

Materials and Methods

Laboratory Animals, Main Reagents and Instruments

This investigation was approved by the Animal Ethics Committee of Shanxi Medical University Animal Center. A total of 30 healthy adult

male Wistar rats weighing 200-220 g were adaptively fed in a suitable environment at (22±2)°C in a 12/12 h light/dark cycle and normally given food and water. They were randomly divided into blank control group (Control group, n=10), DM group (n=10), and miR-135a inhibitor group (n=10). Later, 1% streptozotocin (STZ) solution was prepared using sodium citrate buffer. After fasting for 12 h, the rats in DM and miR-135a inhibitor groups were intraperitoneally injected with STZ at 60 mg/kg to establish the DM model. At 48 h after injection of STZ, blood was sampled from rat tail vein, and the level of blood glucose was determined using a blood glucose meter. The rats with blood glucose >300 mg/L were diagnosed with DM and employed for subsequent research. An equal volume of sodium citrate buffer was intraperitoneally injected in rats of Control group. After 4 weeks, the rats in miR-135a inhibitor group were intraperitoneally injected with miR-135a inhibitor, while those in Control and DM groups with an equal volume of normal saline, and 24 h later, all the rats were sacrificed.

STZ was purchased from Sigma-Aldrich (St. Louis, MO, USA); eosin dyeing solution from Shenyang No.5 Reagent Factory (Shenyang, China); fluorescence quantitative polymerase chain reaction (PCR) reagent and consumables (TaKaRa, Dalian, China); Notch, Notch intracellular domain (NICD), and Hes1 monoclonal antibodies (Santa Cruz Biotechnology; Santa Cruz, CA, USA); synthesized miR-135a inhibitor (Guangzhou RiboBio Co., Ltd., Guangzhou, China); RNA extraction kit (Shanghai Sangon Biotech, Shanghai, China), confocal microscope and fluorescence quantitative PCR amplifier.

Total RNA Extraction and Fluorescence Quantitative PCR

Total RNA was extracted from the renal tissues of rats using TRIzol reagent (Invitrogen, Carlsbad, CA, USA). Then, the absorbance (A) was measured at 260 nm and 280 nm using an ultramicrospectrophotometer, and the ratio of A_{260}/A_{280} represented the concentration and purity of the total RNAs. Qualified RNA samples were reversely transcribed into complementary deoxyribonucleic acid (cDNA). Quantitative reverse transcription (qRT)-PCR amplification was performed using AceQ qPCR SYBR Green Master Mix kit under the following conditions: 95°C for 5 min, followed by 40 cycles at 95°C for 10 s, 60°C for 30 s and 72°C for 1 min, and finally 95°C for 10 min. The fluorescence quantitative PCR

system comprised 5 μ L of PCR Master Mix (2 \times), 1 μ L of PCR reverse primers, 1 μ L of cDNA, and 12 μ L of ddH₂O. Finally, the results were obtained by calculating $2^{-\Delta\Delta Ct}$ (Table I).

Hematoxylin-Eosin (HE) Staining

After being fixed for 24 h, the kidney samples were taken out, washed using clean water, dehydrated in ethanol, embedded in paraffin, and sectioned. Then, the sections were stained with hematoxylin at room temperature for 10 min, washed with clean water for 30 min and acidified in 1% hydrochloric acid for 30 s. After washing in clean water for 30 s, samples were stained with eosin at room temperature for 5 min and dehydrated in ethanol. Finally, the sections were sealed using neutral resin in a ventilated environment, and the changes in the renal tissues of rats were observed under a microscope.

Sirius Red Staining

The kidney fixed for 24 h was obtained, washed using clean water, dehydrated in ethanol, embedded in paraffin, and sectioned. Then, the resulting sections were stained with Celestin blue dye solution at room temperature for 10 min, washed using phosphate-buffered saline (PBS) for 30 min, and stained with Sirius red staining solution at room temperature for 30 min. After washing again with phosphate-buffered saline (PBS) for 30 min, sections were acidified in 1% hydrochloric acid for 5 s, separated using ethanol for 5 s, dehydrated, transparentized, and sealed using neutral resin in ventilated environment. Finally, the changes in the renal tissues of rats were observed under the microscope.

Immunofluorescence Assay

After the rats were sacrificed, the renal tissues were taken out and prepared into frozen sections. The sections were let stand at normal temperature for 15 min, washed using PBS for 3 min \times 3 times, and reacted with 0.3% Triton at room temperature for 10 min. After washing again with PBS for 3

min \times 3 times, sections were blocked using goat serum at 37°C for 45 min, washed using PBS for 3 min, and incubated with the diluted corresponding primary antibodies at 4°C overnight. After PBS washing for 3 min \times 3 times, the sections were incubated with the diluted corresponding secondary antibodies at 37°C for 1 h and washed as above. Cell nuclei were stained with 4',6-diamidino-2-phenylindole (DAPI) for 2 min, and the sections were washed using PBS for 3 min \times 3 times and sealed in 3% glycerol. Finally, the resulting sections were observed under the laser scanning confocal microscope, and images were acquired.

Western Blotting

The rats were sacrificed to remove the kidneys. Tissues were washed with PBS twice, ground in a pre-cooled mortar with liquid nitrogen, added with lysis buffer, and allowed to stand on ice for 1 h, followed by ultrasonic extraction of total protein. Subsequently, the total proteins extracted were centrifuged at 13,000 rpm for 10 min for the supernatant, and the protein concentration therein was determined by the bicinchoninic acid (BCA) assay method (Pierce, Rockford, IL, USA). The same amount of protein sample (30 μ g) was loaded for 12% sodium dodecyl sulphate-polyacrylamide gel electrophoresis (SDS-PAGE). Then, the gels were transferred onto a 0.45 μ m polyvinylidene difluoride (PVDF) membranes (Roche, Basel, Switzerland). The membrane was blocked using 3% bovine serum albumin, washed using PBS with Tween 20 (PBST) twice (5 min/time), incubated with the corresponding primary antibodies diluted by the antibody diluent at 4°C overnight, and washed again with PBST for 5 min \times 3 times. Membranes were incubated with the horseradish peroxidase (HRP) labeled-secondary antibodies diluted by the antibody diluent at 37°C for 1 h. Finally, enhanced chemiluminescence (ECL) fluorescence color development solution was added dropwise for color development and quantification in ChemiDoc MP gel imaging system.

Statistical Analysis

All experiments were performed in triplicate and the results were expressed as mean \pm SD (standard deviation). Statistical Product and Service Solutions (SPSS) 16.0 software (SPSS Inc., Chicago, IL, USA) was used for statistical analysis of data. The results of intergroup comparison were represented as ($\bar{x}\pm s$), and the intergroup comparisons were made *via* one-way analysis of variance (ANOVA), followed by post-hoc test. $p < 0.05$ considered statistically significant differences.

Table I. QRT-PCR primer sequences.

Primer	Sequence
MiR-135a	5' TGCACATCCGTGCAGAGAAT 3' 5' CTGGTTCTGCTTGTTCGC 3'
Notch	5'-CTGTCCCCTGTCAAGCTGAT-3' 5'-CCATCCTGGGTTGTGCTCTT-3'
GAPDH	5' AGGTCGGTGTGAACGGATTTG 3' 5' TGTAGACCATGTAGTTGAGGTCA 3'

Table II. Biochemical parameters of rats.

Group	BG (mmol/L)	GHb (%)	Scr (μ mol/L)	TG (mmol/L)	TC (mmol/L)
Control	5.41 \pm 2.10	1.45 \pm 0.85	13.08 \pm 3.11	1.29 \pm 0.35	2.64 \pm 0.66
DM	38.36 \pm 2.34*	17.81 \pm 1.45*	39.21 \pm 4.21*	2.34 \pm 0.72*	4.06 \pm 0.52*

Note: * p <0.05 vs. Control group. BG: blood glucose, GHb: glycated hemoglobin, Scr: serum creatinine, TG: triglyceride and TC: total cholesterol.

Changes in the Biochemical Parameters of Rats

According to the detection results of the biochemical parameters of rats, those in DM group had substantially raised levels of blood glucose (BG), glycated hemoglobin (GHb), serum creatinine (Scr), triglyceride (TG), and total cholesterol (TC) compared to Control group, and the differences were statistically significant (p <0.05) (Table II).

HE Staining Results of Rat Kidney Tissues

As shown in Figure 1, the rats in Control group had renal tubular cells with normal morphology and clear structure, and no interstitial edema, while those in DM group exhibited evident cavitation in the renal tubular epithelium, evident inflammatory cell infiltration in the renal tubulointerstitium, and distinct tubular expansion.

Sirius Red Staining Results of Rat Kidney Tissues

The red collagen fibers were evenly distributed and lightly stained in the glomeruli and renal tubules of rats in Control group, while the collagen

fibers of the glomeruli and renal tubules of rats in DM group exhibited deep and evident red staining, with evidently disordered and wound nodules. Moreover, compared with those in DM group, the red staining in the glomeruli and renal tubules of rats notably faded and collagen was evenly distributed, with remarkably decreased fibrotic nodules in miR-135a inhibitor group (Figure 2).

Immunohistochemistry Detection Results of Rat Kidney Tissues

According to the observation under a microscope, the brownish-yellow particles presented the positive expression of proteins, and the cell nuclei were stained blue. The detection results showed that both Notch and Hes1 were not expressed in the tubulointerstitial cells and renal tube epithelial cells of rats in Control group, and compared with those in Control group. Positive expressions of Notch and Hes1 in the tubulointerstitial cells, and renal tube epithelial cells of rats were notably enhanced in DM group. Besides, in comparison with those in DM group, their protein levels were remarkably lowered in miR-135a inhibitor group (Figure 3).

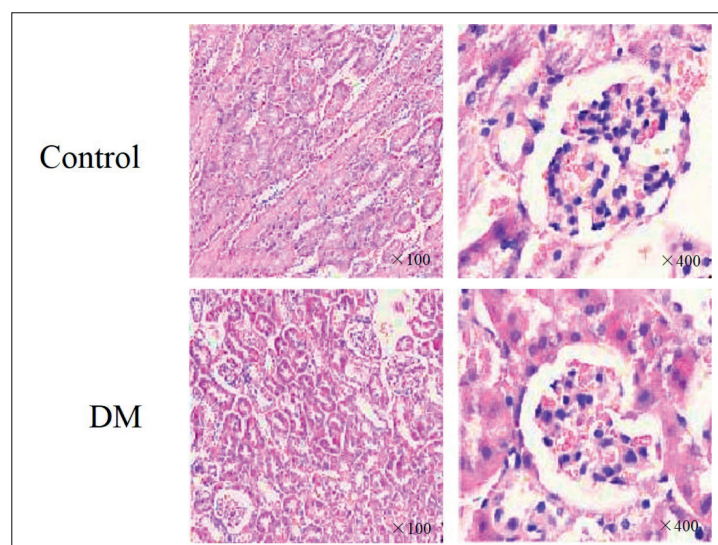


Figure 1. HE staining results of rat kidney tissues (\times 100 and \times 400). Note: Control: Control group and DM: DM group.

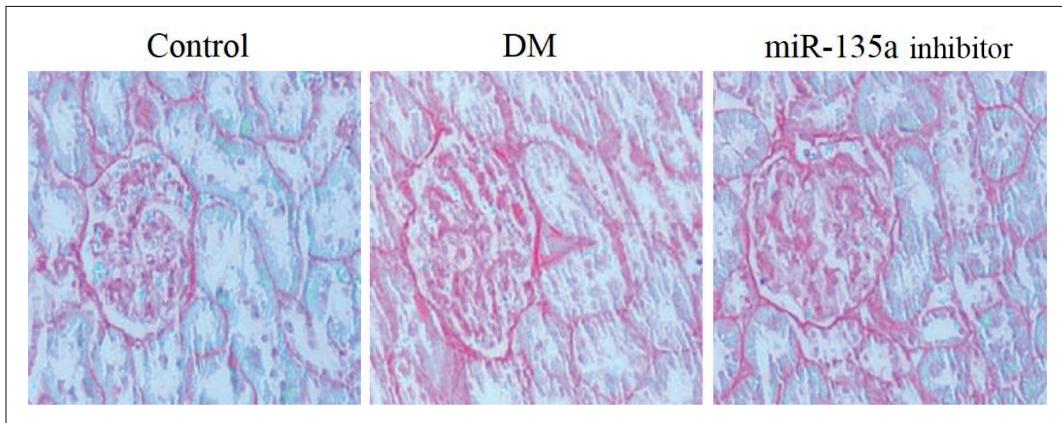


Figure 2. Sirius red staining results of rat kidney tissues ($\times 400$). Note: Control: Control group, DM: DM group, and miR-135a inhibitor: miR-135a inhibitor group.

Protein Expression of Notch in the Renal Tissues of Rats Detected Via Immunofluorescence Assay

It was observed under the laser confocal microscope that Notch was lowly expressed in the rat kidney tissues of Control group, which was mainly expressed in the glomerulus and the minority in the renal tubules. The protein level of Notch in the renal tissues of rats in DM group was considerably higher than that Control group, while its protein expression level in miR-135a inhibitor group was significantly lower than that in DM group (Figure 4).

Expressions of MiR-135a and Notch mRNA in Rat Kidney Tissues

Compared with those in Control group, the mRNA expressions of Notch and miR-135a in the rat kidney tissues were substantially raised in DM group ($p < 0.05$), and they were notably lower in miR-13a inhibitor group than those in DM group ($p < 0.05$) (Figure 5).

Protein Expressions of Notch, NICD, and Hes1 in Rat Kidney Tissues

As showed in Figure 6, the protein levels of Notch and the downstream NICD and Hes1 in the renal tissues of rats in DM group were consider-

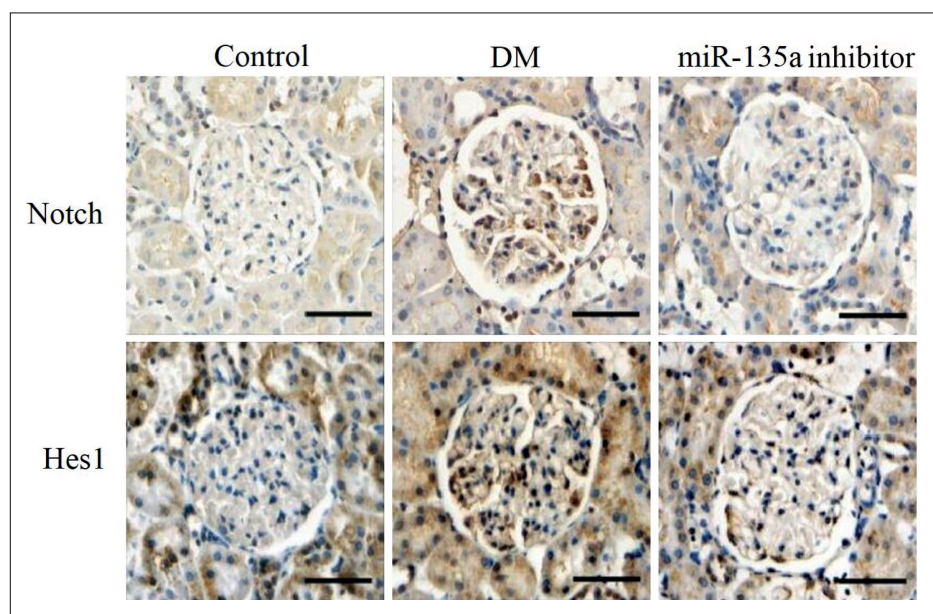


Figure 3. Protein expressions of Notch and Hes1 in rat kidney tissues ($\times 600$). Note: Control: Control group, DM: DM, and miR-135a inhibitor: miR-135a inhibitor group.

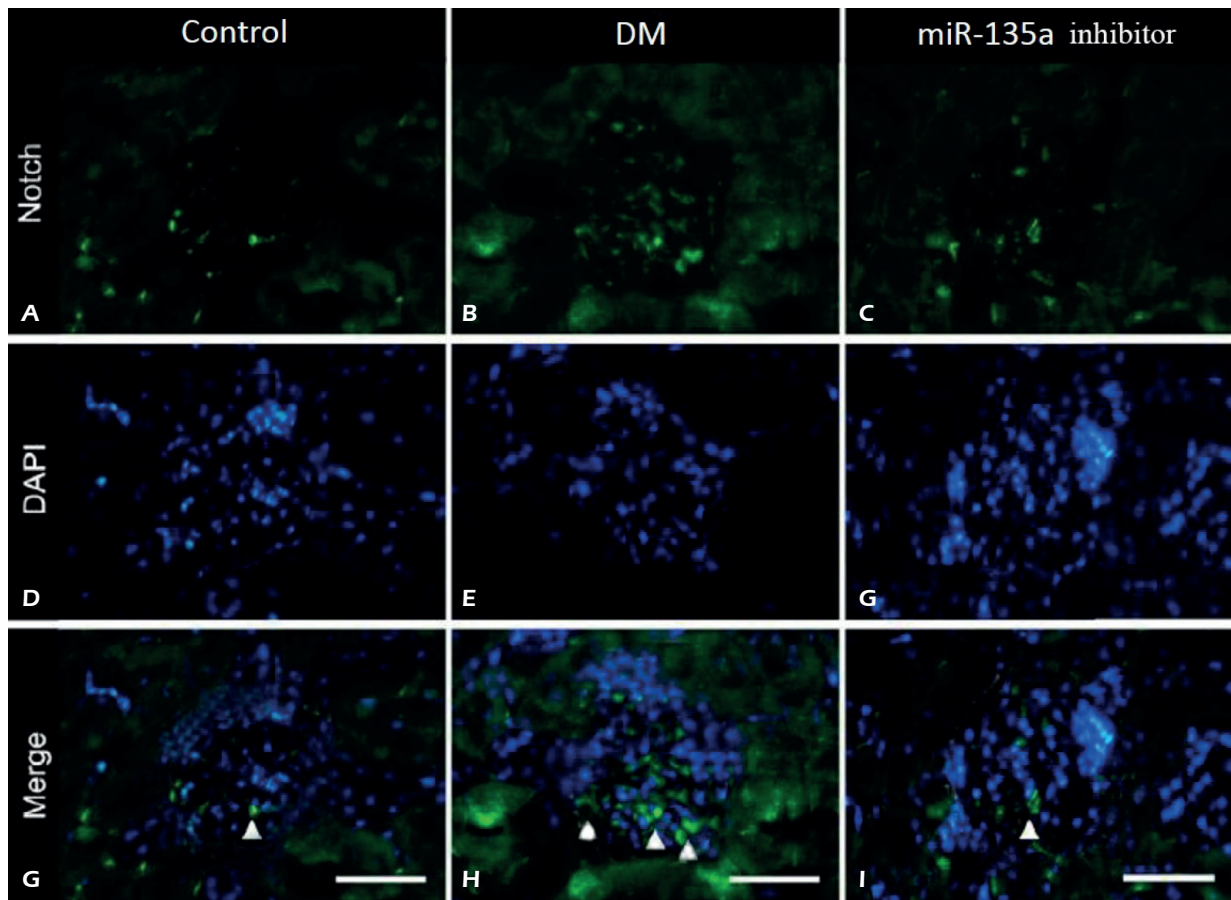


Figure 4. Protein expression of Notch in rat kidney tissues ($\times 800$). Note: Control: Control group, DM: DM group, and miR-135a inhibitor: miR-135a inhibitor group.

ably higher than those in Control group ($p < 0.05$). Their protein levels in miR-135a inhibitor group were markedly lower than those in DM group ($p < 0.05$) (Table III).

Discussion

DM has become a chronic metabolic disease that endangers the health of people in the world.

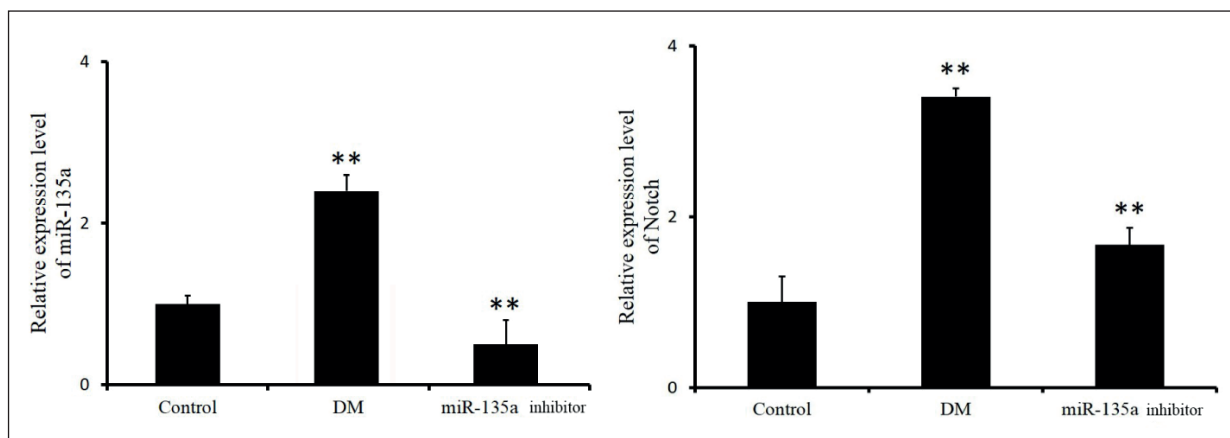


Figure 5. Expressions of miR-135a and Notch mRNA in rat kidney tissues in each group. Note: Control: Control group, DM: DM group, and miR-135a inhibitor: miR-135a inhibitor group. ** $p < 0.01$ vs. Control group.

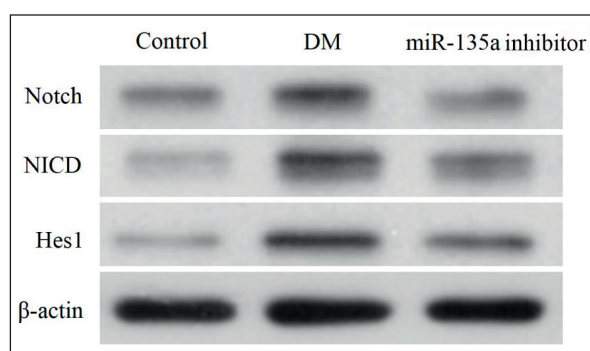


Figure 6. Protein expressions of Notch, NICD and Hes1 in rat kidney tissues. Note: Control: Control group, DM: DM group, and miR-135a inhibitor: miR-135a inhibitor group.

According to the statistics of the International Diabetes Federation (IDF), the number of DM patients worldwide increases year by year and is expected to exceed 552 million by 2035¹¹. DM can cause microvascular lesions, resulting in DKD that occurs in 30-47% of end-stage nephropathy cases¹². The pathogenesis of DKD has not yet been fully clarified. According to the findings in a study, the progression of DKD is correlated with high blood glucose¹³. Strictly controlling blood glucose can slow down the progression of DKD and improve the renal function of DM patients¹⁴. Although blood glucose is controlled, the DM patients will ultimately experience end-stage nephropathy. High blood glucose can induce stress responses in the kidneys, such as endoplasmic reticulum stress, oxidative stress, mitochondrial dysfunction, and inflammation response, ultimately resulting in glomerulosclerosis¹⁵.

MiRNAs, conservative small non-coding RNAs, inhibit the translation of proteins at post-transcription level through complementary base pairing, and the development of multiple diseases is closely associated with the aberrant expressions of miRNAs¹⁶. The family of

miR-135, located on human chromosome, consists of miR-135a and miR-135b¹⁷, and miR-135 affects the development and progression of various diseases. In a study¹⁸ conducted in 2015, it was found that miR-135 played vital roles in the early diagnosis, targeted gene therapy, and prognosis judgment of various tumors. Another study¹⁹ demonstrated that miR-135a is up-regulated in the serum of DM patients, suggesting its potential as a marker of DM.

In the present study, DM model in rats was constructed by STZ administration, and DM rats were injected with miR-135a inhibitor to explore the influence of miR-135a on the Notch pathway. The detection results of the biochemical parameters of DM rats revealed that the BG, GHb, Scr, TG, and TC were all elevated considerably in DM group ($p < 0.05$). HE staining showed that rats in DM group exhibited evident cavitation in renal tubular epithelium, evident inflammatory cell infiltration in the renal tubulointerstitium, and distinct tubular expansion, illustrating that the DM rat model was successfully established. After injection of miR-135a inhibitor, the collagen in the renal tissues of DM rats was evenly distributed with notably alleviated fibrous nodules, which was in agreement with the previous study²⁰. Moreover, the immunohistochemistry detection results showed that the protein expression of Notch declined markedly. According to the results of the qRT-PCR, the mRNA level of Notch was remarkably lowered after knock-down of miR-135a ($p < 0.05$). Finally, protein levels of NICD, and Hes1 in the downstream of the Notch signaling pathway were detected *via* Western blotting. It was found that the protein expressions of Notch, NICD, and Hes1 were notably lowered after the inhibition of miR-135a. In summary, inhibition of miR-135a can reduce the renal fibrosis in DM rats through the Notch pathway.

However, the specific mechanism of the influence of miR-135a on fibrosis may be asso-

Table III. Optical density (OD) of protein bands of Notch, NICD and Hes1 in each group.

Protein	OD	Control	DM	MiR-135a inhibitor
Notch	Target protein/ β -actin	0.84 \pm 0.24	4.83 \pm 0.33 ^a	1.46 \pm 0.44 ^{ab}
NICD	Target protein/ β -actin	0.52 \pm 0.21	2.95 \pm 0.34 ^a	1.68 \pm 0.31 ^{ab}
Hes1	Target protein/ β -actin	0.34 \pm 0.29	3.82 \pm 0.34 ^a	1.28 \pm 0.28 ^{ab}

Note: Control: Control group, DM: DM group, and miR-135a inhibitor: miR-135a inhibitor group. ^a $p < 0.05$ vs. Control group, and ^b $p < 0.05$ vs. DM group.

ciated with other target genes of miR-135a as well. One report²¹ demonstrated that the level of miR-135a rises in the skeletal muscle in human DM, and miR-135a over-expression weakens the insulin-stimulated phosphorylation and activation of PI3Kp85 α , as well as glucose uptake *via* the IRS2/Akt signaling pathway. Based on the results Zeng et al²², miR-135a regulates several target genes, including MTSS1, HOXA10, SMAD5, and JAK2. This research only verified the influence of miR-135a on the Notch signaling pathway, and failed to elucidate the potential involvement of another signaling pathway. Our findings lay an experimental foundation for the subsequent further research on the pathogenesis of renal fibrosis in DM.

Conclusions

In summary, inhibition of miR-135a can relieve the renal fibrosis in DKD rats through the Notch pathway.

Funding Acknowledgements

National Natural Science Foundation Grant (No. 81700283).

Conflict of Interests

The Authors declare that they have no conflict of interests.

References

- XU Y, WANG L, HE J, BI Y, LI M, WANG T, WANG L, JIANG Y, DAI M, LU J, XU M, LI Y, HU N, LI J, MI S, CHEN CS, LI G, MU Y, ZHAO J, KONG L, CHEN J, LAI S, WANG W, ZHAO W, NING G; 2010 China Noncommunicable Disease Surveillance Group. Prevalence and control of diabetes in Chinese adults. *JAMA* 2013; 310: 948-959.
- ISMAIL-BEIGI F, CRAVEN T, BANERJI MA, BASILE J, CALLES J, COHEN RM, CUDDIHY R, CUSHMAN WC, GENUTH S, GRIMM RJ, HAMILTON BP, HOOGWERF B, KARL D, KATZ L, KRICKORIAN A, O'CONNOR P, POP-BUSUI R, SCHUBART U, SIMMONS D, TAYLOR H, THOMAS A, WEISS D, HRAMI-*AK* I; ACCORD trial group. Effect of intensive treatment of hyperglycaemia on microvascular outcomes in type 2 diabetes: an analysis of the ACCORD randomised trial. *Lancet* 2010; 376: 419-430.
- THOMAS MC, BROWNLEE M, SUSZTAK K, SHARMA K, JANDELEIT-DAHME KA, ZOUNGAS S, ROSSING P, GROOP PH, COOPER ME. Diabetic kidney disease. *Nat Rev Dis Primers* 2015; 1: 15018.
- DE ZEEUW D. Albuminuria: a target for treatment of type 2 diabetic nephropathy. *Semin Nephrol* 2007; 27: 172-181.
- MA R, LIU L, LIU X, WANG Y, JIANG W, XU L. Triptolide markedly attenuates albuminuria and podocyte injury in an animal model of diabetic nephropathy. *Exp Ther Med* 2013; 6: 649-656.
- GAO Q, SHEN W, QIN W, ZHENG C, ZHANG M, ZENG C, WANG S, WANG J, ZHU X, LIU Z. Treatment of db/db diabetic mice with triptolide: a novel therapy for diabetic nephropathy. *Nephrol Dial Transplant* 2010; 25: 3539-3547.
- DONG XG, AN ZM, GUO Y, ZHOU JL, QIN T. Effect of triptolide on expression of oxidative carbonyl protein in renal cortex of rats with diabetic nephropathy. *J Huazhong Univ Sci Technolog Med Sci* 2017; 37: 25-29.
- JEFFERSON JA, SHANKLAND SJ, PICHLER RH. Proteinuria in diabetic kidney disease: a mechanistic viewpoint. *Kidney Int* 2008; 74: 22-36.
- DING Y, CHOI ME. Autophagy in diabetic nephropathy. *J Endocrinol* 2015; 224: R15-R30.
- LI XY, WANG SS, HAN Z, HAN F, CHANG YP, YANG Y, XUE M, SUN B, CHEN LM. Triptolide restores autophagy to alleviate diabetic renal fibrosis through the miR-141-3p/PTEN/Akt/mTOR pathway. *Mol Ther Nucleic Acids* 2017; 9: 48-56.
- SEN S, CHAKRABORTY R. Treatment and diagnosis of diabetes mellitus and its complication: advanced approaches. *Mini Rev Med Chem* 2015; 15: 1132-1133.
- LIU G, SUN Y, LI Z, SONG T, WANG H, ZHANG Y, GE Z. Apoptosis induced by endoplasmic reticulum stress involved in diabetic kidney disease. *Biochem Biophys Res Commun* 2008; 370: 651-656.
- BROWNLEE M. Biochemistry and molecular cell biology of diabetic complications. *Nature* 2001; 414: 813-820.
- KIM M, PARK Y, KWON Y, KIM Y, BYUN J, JEONG MS, KIM HU, JUNG HS, MUN JY, JEOUNG D. MiR-135-5p-p62 axis regulates autophagic flux, tumorigenic potential, and cellular interactions mediated by extracellular vesicles during allergic inflammation. *Front Immunol* 2019; 10: 738.
- SODROSKI C, LOWEY B, HERTZ L, JAKE LT, LI Q. MicroRNA-135a modulates hepatitis C virus genome replication through downregulation of host antiviral factors. *Virology* 2019; 34: 197-210.
- ZHANG Y, REN S, YUAN F, ZHANG K, FAN Y, ZHENG S, GAO Z, ZHAO J, MU T, ZHAO S, SHANG A, LI X, JIE Y. MiR-135 promotes proliferation and stemness of oesophageal squamous cell carcinoma by targeting RERG. *Artif Cells Nanomed Biotechnol* 2018; 46: 1210-1219.
- VIDAL AF, CRUZ AM, MAGALHAES L, PEREIRA AL, ANAIS-*SI* AK, ALVES NC, ALBUQUERQUE PJ, BURBANO RM, DEMACHKI S, RIBEIRO-DOS-SANTOS A. hsa-miR-29c and hsa-miR-135b differential expression as potential biomarker of gastric carcinogenesis. *World J Gastroenterol* 2016; 22: 2060-2070.

- 18) LI D, DENG T, LI H, LI Y. MiR-143 and miR-135 inhibitors treatment induces skeletal myogenic differentiation of human adult dental pulp stem cells. *Arch Oral Biol* 2015; 60: 1613-1617.
- 19) DiNICOLANTONIO JJ, McCARTY M. Autophagy-induced degradation of Notch1, achieved through intermittent fasting, may promote beta cell neogenesis: implications for reversal of type 2 diabetes. *Open Heart* 2019; 6: e001028.
- 20) HE F, PENG F, XIA X, ZHAO C, LUO Q, GUAN W, LI Z, YU X, HUANG F. MiR-135a promotes renal fibrosis in diabetic nephropathy by regulating TRPC1. *Diabetologia* 2014; 57: 1726-1736.
- 21) HUANG KC, CHUANG PY, YANG TY, HUANG TW, CHANG SF. Hyperglycemia inhibits osteoblastogenesis of rat bone marrow stromal cells via activation of the Notch2 signaling pathway. *Int J Med Sci* 2019; 16: 696-703.
- 22) ZENG YB, LIANG XH, ZHANG GX, JIANG N, ZHANG T, HUANG JY, ZHANG L, ZENG XC. miRNA-135a promotes hepatocellular carcinoma cell migration and invasion by targeting forkhead box O1. *Cancer Cell Int* 2016; 16: 63.